Investigations on Iron Precipitates accumulating from underground workings and Mud Lake at South Bay

Prepared for

Boojum Research Ltd.

By

Dr. G. Meinrath
RER Consultants Passau, Schießstattweg 3a D-94032 Passau, Germany

Table of contents

List of Tables

List of Figures

List of Maps

1. Introduction

In pyritic mining wastes, the release and subsequent oxidation of Fe(II) from mining sites may produce non-negligible amounts of high sulfate and extremely low pH waters. The resulting acid mine drainage (AMD) may be divided into three types:

- iron sulfide oxidation,
- dissolution of soluble iron sulfate minerals, and
- the dissolution of less soluble sulfate minerals of the alunite-jarosite series.

The oxidation of iron sulfide minerals such as pyrite (FeS_2) and pyrrhotite is responsible for the majority of acid production from mining wastes. In addition to metals, acid, sulfate is also released to ground and surface water. If sulfate is present in higher concentrations a variety of iron minerals may form, i.e.:

- jarosite ($XFe_3(SO_4)_2(OH)_6$, (X being a monovalent cation)
- Schwertmannite ($Fe_8O_8(OH)_6SO_4$).

These secondary minerals are not stable and the release of sulfate by dissolution of these minerals may result in the formation of Fe(III) hydroxides with subsequent acid (H^+) release.

Secondary mineral formation, with hydrogen-ion generation leading to pH values as low as pH 1, was reported in stored South Bay tailings pore water. Investigations on the secondary mineral phases, along with microbial investigations, were carried out and Schwertmannite minerals were detected as reported in Kalin, 2003, "*The acid generation potential of iron precipitates and their sludge in Decommissioning with Ecological Engineering*". This is a matter of some concern, given the high number of hydrogen ions, generated by the formation of Schwertmannite, The natural precipitation of stable, iron-hydroxide sludge, which is not a source of acidity, is an important component of the Ecological Engineering decommissioning approach. Thus Schwertmannite formation is undesirable, and the conditions under which it occurs must well understood. Samples of sludge were collected from relevant locations at the South Bay site for an investigation into the formation of this secondary mineral.

2.0 Site description and sample collection

Samples of iron hydroxide sludge were gathered from a constructed ditch that carries effluents from the undergrounds workings, emerging at the Backfill Raise to Boomerang Lake, from Mud Lake outflow into Armanda Lake (Map 1 a and Map 1b) and from effluent emerging out of waste rock at the Warehouse Seep on the mine site. These were investigated for the presence of Schwertmannite.

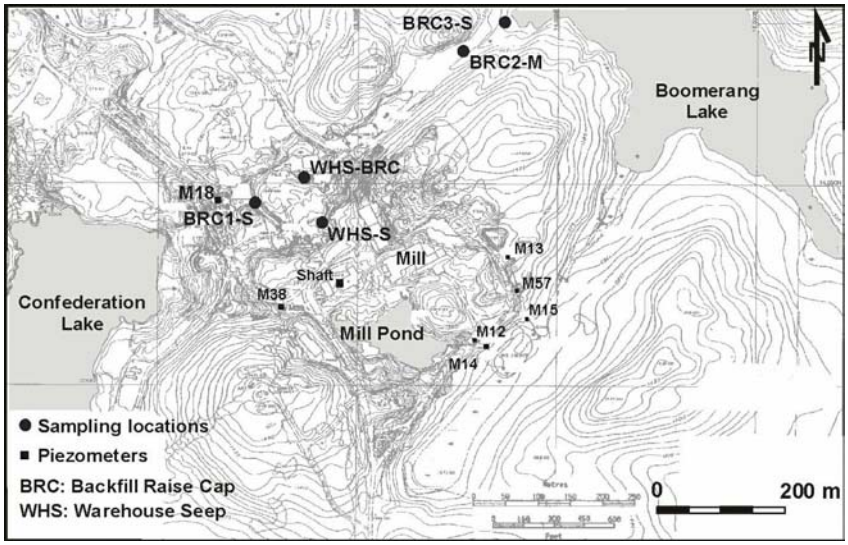

Map 1a: Mine Site

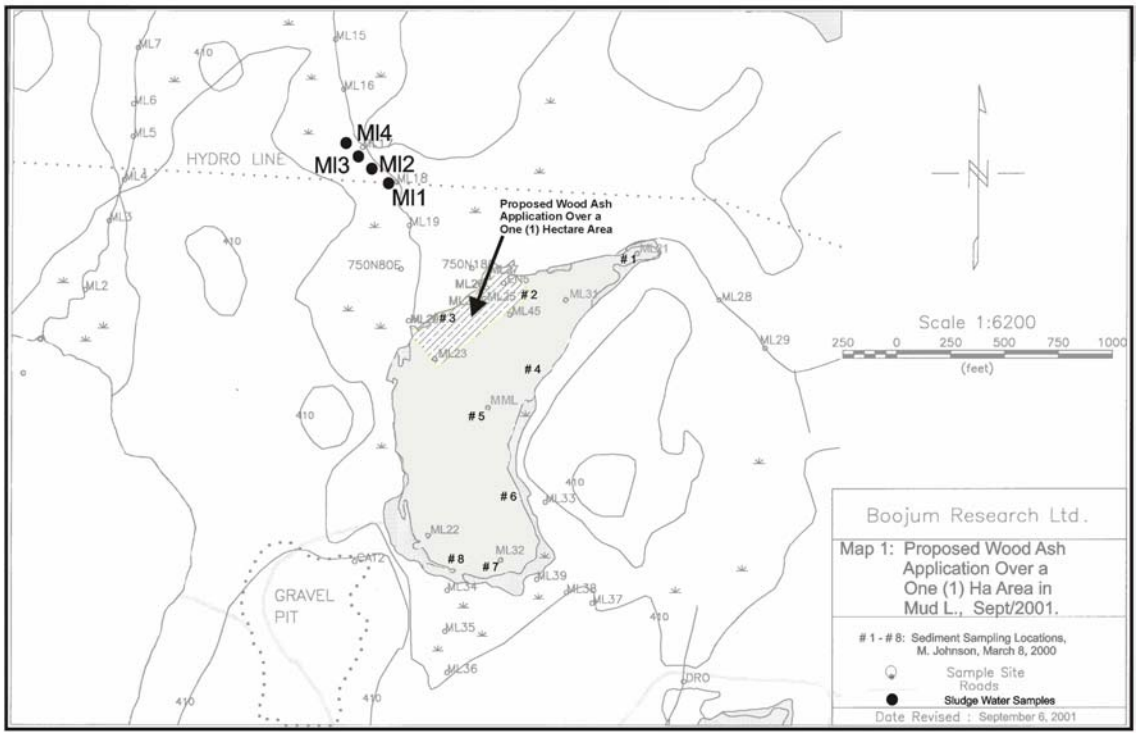

Map 1b: Mud Lake outflow

2.1 Analytical procedure

A total of 22 sediment samples were shipped (Table 1a and Table 1b) to the Technische Universität Bergakademie Freiberg, Institute of Geology. The samples were sealed in centrifuge tubes (50 mL).

Table 1a: Description of the sampling locations for sludge from Mud lake outflow area

Designator	Field pH	Location	Colour (precipitate)
ML1-F	**2.6_4** [a)]	**at ML 18**	**reddish brown**
ML1-S	2.6_4	at ML 18	reddish brown
ML1-D	**2.6_4**	**at ML 18**	**Dark brown**
ML2-F	**2.6_4**	**25 m upstream ML 18**	**reddish brown**
ML2-S	2.6_4	25 m upstream ML 18	yellow brown
ML2-D	2.6_4	25 m upstream ML 18	umbra (dark brown)
ML3-F	**2.6_4**	**anti-beaver culverts**	**reddish brown**
ML3-S	2.6_4	anti-beaver culverts	yellow brown
ML3-D	2.6_4	anti-beaver culverts	reddish brown
ML4-F	2.6_4	south end of beaver dam	reddish brown
ML4-S	2.6_4	south end of beaver dam	greenish grey
ML4-D	2.6_4	south end of beaver dam	umbra (dark brown)

Table 1b: Description of the sampling locations for sludge from the mine site.

Designator	pH	Location	Colour (precipitate)
BRC1-S	6.4_2	10 m below BRC outfall	reddish brown
BRC1-S***	6.4_2	10 m below BRC outfall	yellow brown
BRC2-M	3.1_6	5 m upstream of BR2.5	yellow brown
BRC2-M*	**3.1_6**	**5 m upstream of BR2.5**	**Reddish brown**
BRC3-S	3.1_6	ditch at boomerang Lake	yellow grey
BRC3-D-	3.1_6	Ditch at Boomerang Lake	reddish brown
WHS-S-W	3.3_8	below WHS outfall pipe	black
WHS-S-D	3.3_8	below WHS outfall pipe	black
WHS-M	3.3_8	above culvert at BR ditch	umbra (dark brown)
WHS- BRC**	**3.3_8**	**above culvert at BR ditch**	**Reddish brown**

Note: F= flowing water, D= dry above stream edge, S= stagnant, M = in flow path

a) subscript not significant value
* mislabelled should be dry D
** mislabelled should be dry D
*** mislabelled should be dry D
Bolded = power X-ray diffraction

The field pH values, measured when the sludge was collected from the Mud Lake outflow area, was consistently around 2.6 with a Eh value of 650 mV at a temperature of 14.5 ^{o}C. For the samples from the mine site from the backfill raise and the Warehouse seep the pH varied. The pH immediately below the discharge area of the effluent from the underground workings was 6.4, with a low Eh of 80 mV. As the water flowed through the ditch towards Boomerang Lake, oxidation occurred, resulting in a pH of 3.1. The second source of sludge on the mine site collected originating from Warehouse Seep (WHS) is an effluent which has already oxidized as it travels through the pyritic waste rock used for fill during mill construction and emerges as pH 3.3 with an Eh of 510mV.

Supernatant water that was contained in all shipped samples was studied by ion chromatography for sulfate concentration. An aliquot of the solid was oven dried and the iron phases dissolved by hydrochloric acid. Sulfate was separated from iron by precipitating iron hydroxide with ammonia. The amount of sulfate in the sludge was determined by turbidity measurement after precipitation as $BaSO_4$. Components other than sulfate have not been analysed to date.

Iron hydroxides, oxyhydroxides and oxides as well as the sulphate-containing phases jarosite and Schwertmannite (with idealized stoichiometric formulas given above) generally form poorly crystalline phases in nature. It is possible to analyse the trace minerals in these phases (by X-ray crystallography and a full-fledged mineralogical analysis including leaching of the sludges by acetone to separate iron precipitate from larger particles (e.g. sand), microscopic analysis and Raman spectroscopy) but the small amounts of minerals involved to do justify the expense of such procedures. Such minor amounts are irrelevant to the restoration of the site. Schwertmannite, which is of greater concern, can be reliably determined by using X-ray powder diffraction.

3. Results

The supernatant analysis is presented in Table 2a for Mud Lake and in Table 2b for the sludge on the mine site. Initially, three samples (BRC2D, WHS-BRC-D and ML1-D) were selected based on their colour appearance, and submitted to X-ray powder diffraction. Concurrently, sulphate analysis of the supernatant was carried out on all samples where sufficient water was available. Subsequently two more samples were submitted to X-ray powder diffraction, ML1-F with high sulphate content in the solids and ML3-F, with lower sulphate content. It is generally believed, that a combination of high Fe and sulphate is promoting Schwertmannite formation.

Table 2a: Sulphate content of supernatant water and solid sludge: Mud Lake outflow area

Designator	Supernatant $SO_{4(aq)}$ [mol L^{-1}]	Solids $SO_{4(s)}$ [g kg^{-1}]	X-ray performed
ML1-F	0.02	80 g	X
ML1-S	0.032	0.4 g	
ML1-D	n.d.	n.d.	X
ML2-F	0.02	1.8	X
ML2-S	0.05	0.6	
ML2-D	n.d.	5.3	
ML3-F	0.035	14.4	X
ML3-S	0.12	n.d.	
ML3-D	0.23	20	
ML4-F	n.d.	0.8	
ML4-S	0.056	n.d.	
ML4-D	n.d.	1.8	

Note: n.d. = not determined, insufficient liquid in supernatant.

Table 2b: Sulphate content of supernatant water and solid sludge: underground workings on the mine site.

Designator	Supernatant $SO_{4(aq)}$ [mol L^{-1}]	Solid $SO_{4(s)}$ [g kg^{-1}]	X-ray
BRC1-S	0.035	0.03	
BRC1-S***	n.d.	1.5	
BRC2-M	0.05	0.0	
BRC2-M*	n.d.	n.d.	X
BRC3-S	0.1	0.01	
BRC3-D	n.d.	0.01	
WHS-S-wet	0.2	9.1	
WHS-S-dry	n.d.	0.07	
WHS	0.3	0.16	
WHS-BRC**	n.d.	n.d.	X

* mislabelled should be dry D
** mislabelled should be dry D
*** mislabelled should be dry D

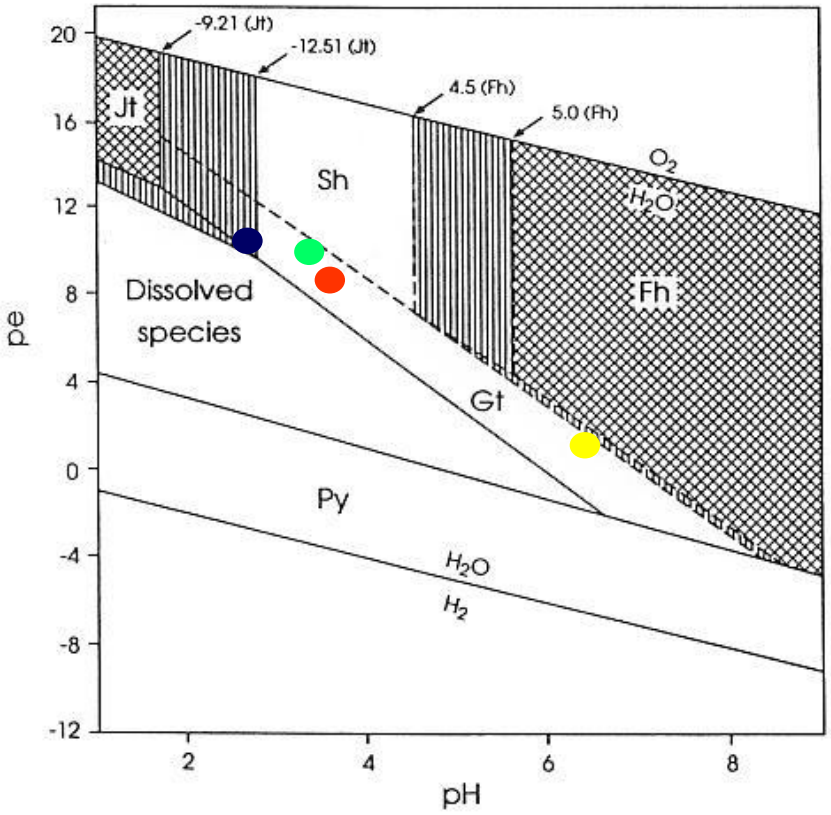

FIG. 10. pe-pH diagram for Fe–S–K–O–H system at 25°C where pe = Eh(mv)/59.2; total log activities of Fe^{2+} = −3.47; Fe^{3+} = −3.36 or −2.27); SO_4^{2-} = −2.32, K^+ = −3.78; log K_{so} values for solid phases as given in Fig. 6. Jt = K-jarosite, Sh = schwertmannite, Fh = ferrihydrite, Gt = goethite, Py = pyrite. Line equations are: Gt (pe = 17.9–3 pH); Jt (pe = 16.21–2 pH); Fh (pe = 21.50–3 pH), Sh (pe = 19.22–2.6 pH), and Py (pe = 5.39–1.14 pH). Fields of metastability shown by dashed lines. Single-hatched areas demonstrate expansion of K-jarosite and ferrihydrite fields if lower log K_{so}'s are selected.

Figure 1: Phase diagram copied from Bigham et al. (1996).

Blue: approximate location of the ML samples
Yellow: approximate location of the BRC1 samples
Green: approximate location of the other BRC samples
Red: approximate location of the WHS samples

The conditions under which the stability diagram is strictly valid (solubility products of solid phases, activities of total Fe(II), Fe(III), sulfate and potassium content)are defined by the authors. The authors assumed lower sulfate concentrations, by about an order of magnitude, to construct the phase diagram, namely $4.8 \cdot 10^{-3}$ mol L^{-1}. From the analysis of the supernatant, the concentration in the South Bay samples is much higher with values of above $2 \cdot 10^{-2}$ mol L^{-1}. Hence, the stability field of Schwertmannite and jarosite would be a bit larger.

Yu et al. (1999) estimated a solubility product of Schwertmannite lower than Bigham et al. (1996). From the pH /E_H values measured in the field this suggests that Schwertmannite formation is possible in the Mud Lake sludges

This initial assessment suggests that phase diagrams must be interpreted with caution. It is unknown whether Bigham et al. have taken into account complexation effects when calculating stability limits for the solid phases. The sulfate concentrations in the South Bay samples of the supernatants vary but are generally higher than assumed by Bingham in his stability field diagram. Further consideration must be given to potassium concentrations, which have not been determined for these samples. Generally the literature indicates the existence of a large number of solubility products for the various iron solid phases. Other data would result in different stability fields.

For example, Yu et al. (1999) suggest a solubility product for Schwertmannite of 10.5 ± 2.5 in contrast to 18 ± 2.5 of Bigham et al. (1996). The question is whether the difference is actually significant. A Ljungskile calculation (Ödegaard-Jensen et al. 2004) takes into account the uncertainty in the aqueous species' constants. Stability field diagram of poorly soluble phases are often calculated without reference to the solution chemistry. But a solubility curve, as presented in Fig. 2, is calculated from the solubility product and the formation constants of solution species. The relevant species and the applied uncertainties are given in Table 3.

Table 3: Thermodynamic data and estimated uncertainties applied in the calculation of Fig.2

Species	Thermodynamic constant lg K°	Uncertainty (1 σ)
$Fe(OH)^+$	-9.50	0.25
FeCO3	4.38	0.12
$Fe(OH)^{2+}$	-2.05	0.5
$Fe(OH)_2^+$	-6.35	0.25
$Fe(OH)_3$	-13.45	0.3
$Fe(OH)_4^-$	-21.43	0.2
$Fe_2(OH)_2^{4+}$	-2.90	0.2

Source: JESS thermodynamic data base [4]

If the 95% confidence limits of two distributions overlap only slightly, then it is difficult to make a clear statistical statement. In other words: we cannot clearly say whether the distributions are significantly different or not.

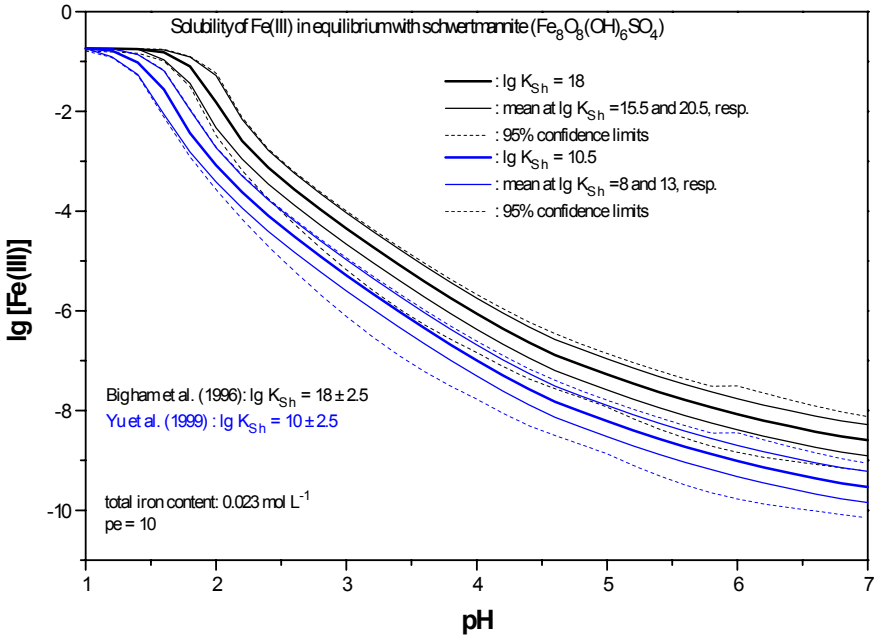

Figure. 2: Comparison of Schwertmannite solubility for lg K_{Sh} = 18 ± 2.5 (Bigham et al. 1996) and lg K_{Sh} = 10.5 (Yu et al. 1999).

The black curves in Figure 2 represent Bigham et al. data. The central line gives the mean value solubility. The upper solid curve represents the solubility for the higher value of the solubility product. The upper dashed line represents the 95% confidence limit. The respective data are given for the black lower curves. The blue lines correspond to Yu et al. data. The numerically big difference in the K_{Sh} values as presented both by Bigham et al. and Yu et al. are reduced to insignificance in the Schwertmannite solubility calculations. In assessing their values, both Yu and Bingham have neglected significant error contributions.

Although the phase diagram would allow the interpretation that Schwertmannite might form, the above discussion elucidates some of the problems associated with this conclusion. Most importantly, it has to be concluded that the presence or absence of Schwertmannite in the South Bay samples cannot be assessed from the phase diagram using pH/Eh and water composition alone. In summary, it may be misleading to compare experimental data and predicted behaviour merely on the basis of the mean values of respective parameters. Powder X-ray analysis is required to ascertain, with some degree of certainty, the presence or absence of the Schwertmannite in the South Bay sludge accumulations.

3.2 X-ray powder data

In Figures 3 a to 3 f the results are presented for each sample. Note that the horizontal scale is not the same for each figure. The general pattern when the individual spectra are different. The two most similar once are ML2F and ML3F, both sludges from Mud lake.

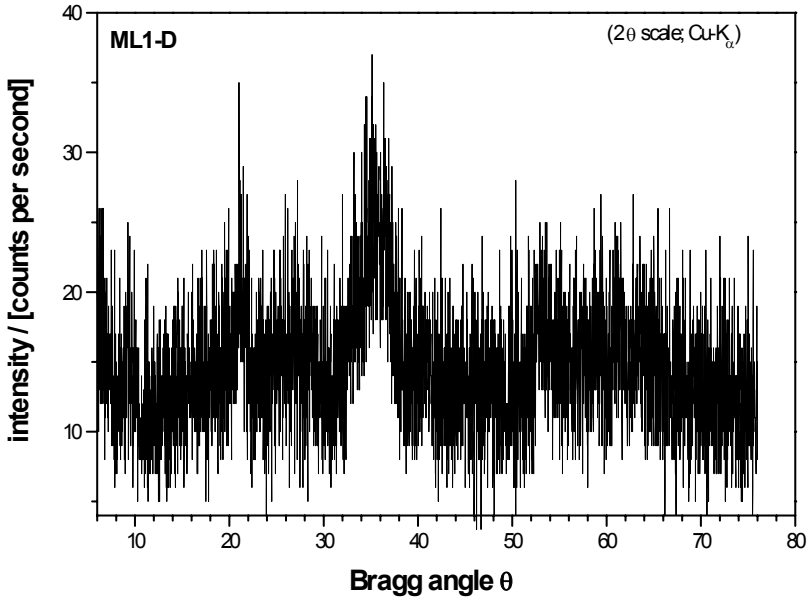

Figure 3a: X-ray data for ML1-D sample

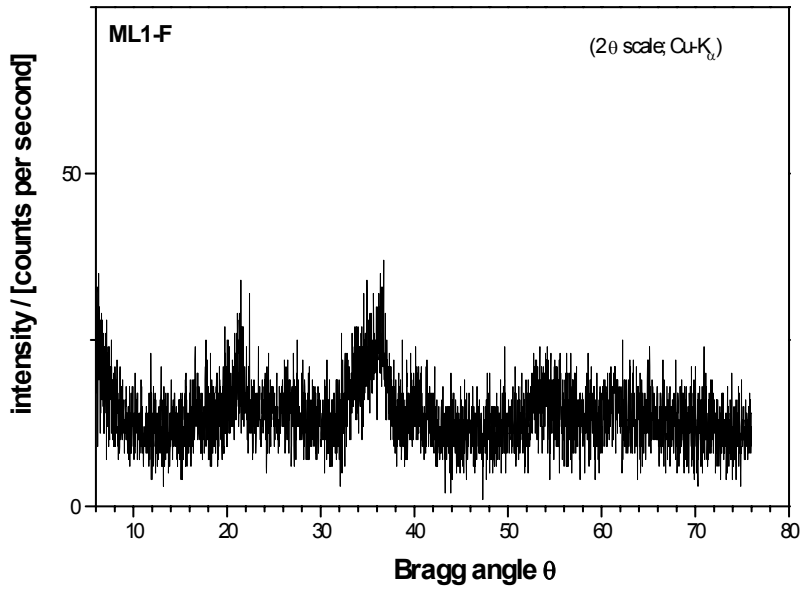

Figure 3b: X-ray data for ML1-F sample

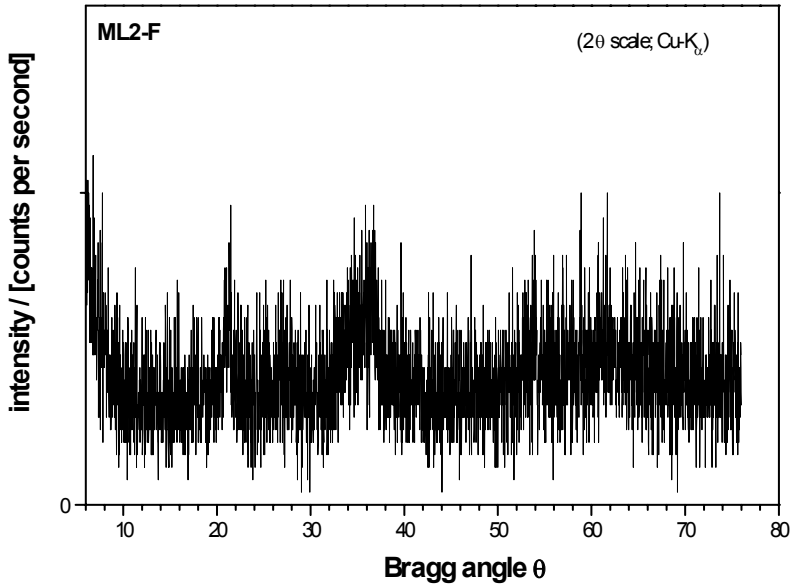

Figure 3c: X-ray data for ML2-F sample

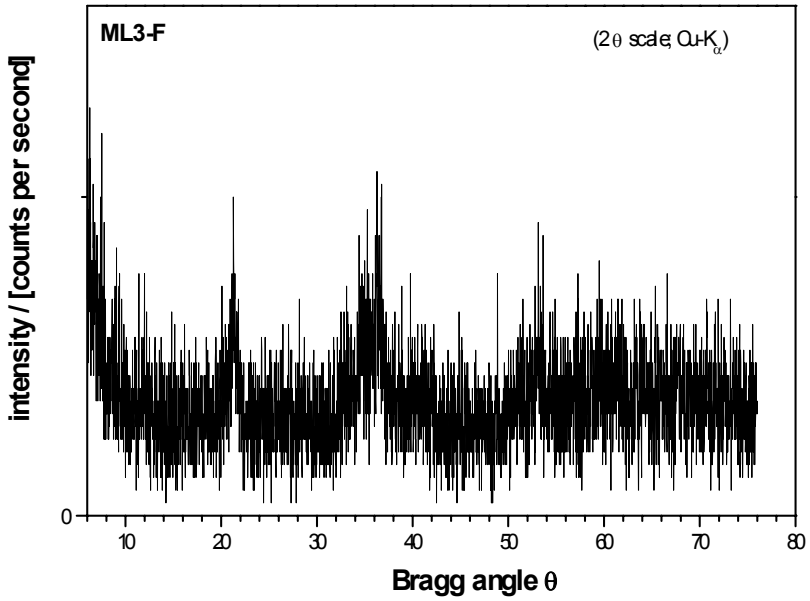

Figure 3d: X-ray data for ML3-F sample

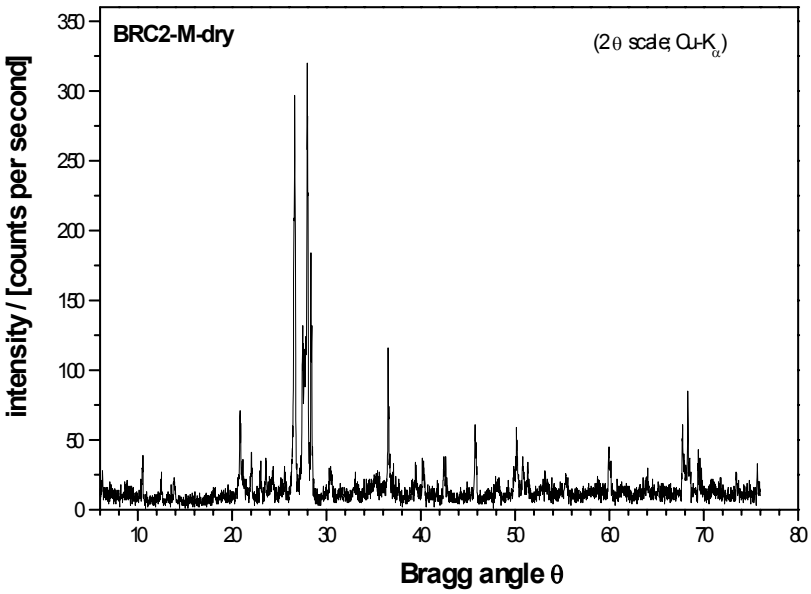

Figure 3e: X-ray data for BRC2-M-dry sample

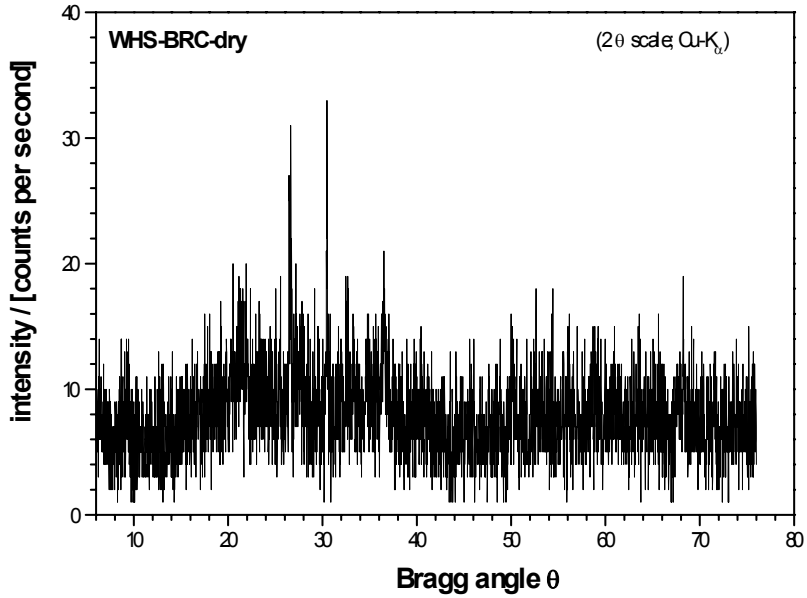

Figure 3f: X-ray data for WHS-BRC-dry sample

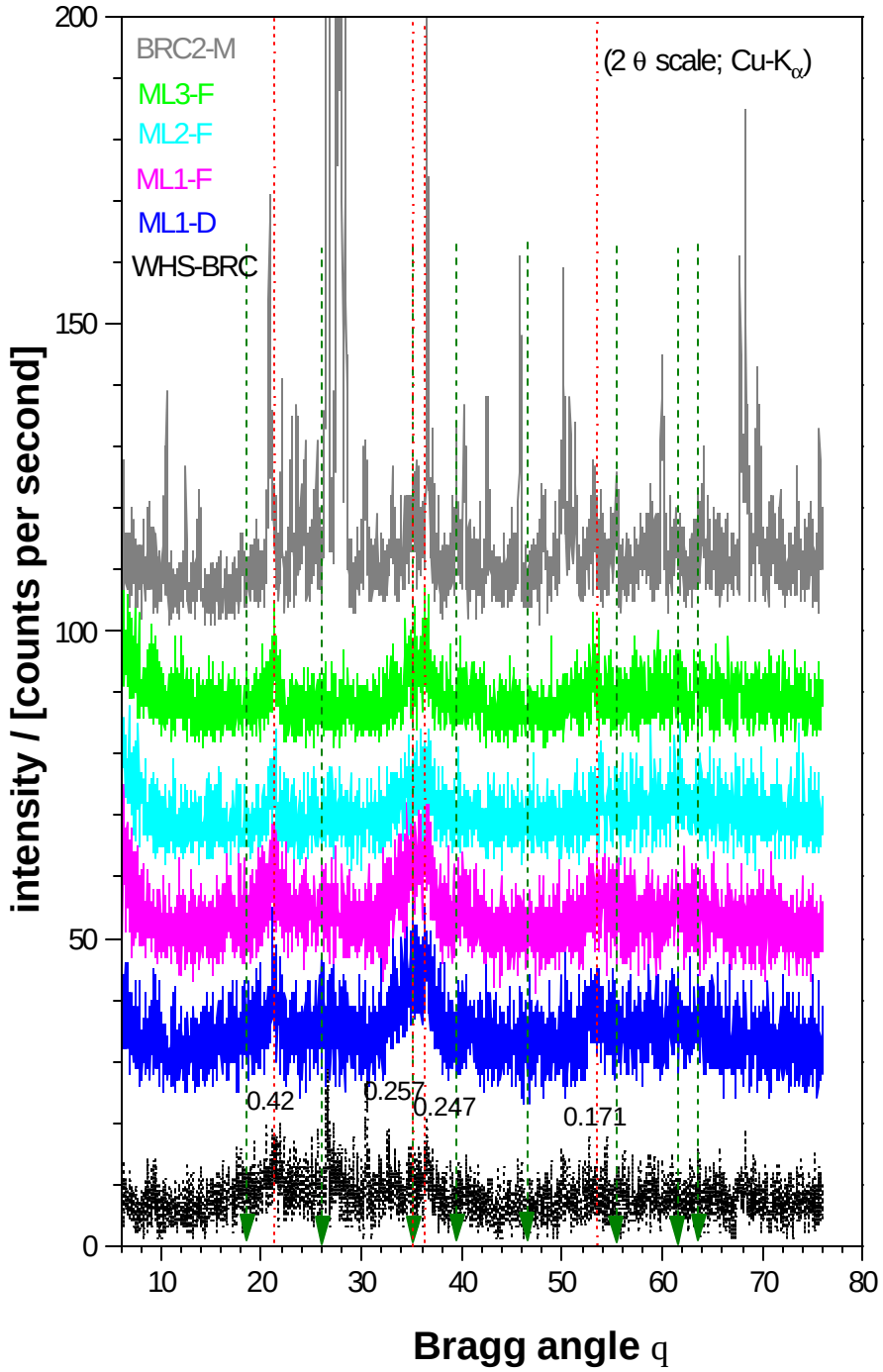

Figure 4: A comparison of the six X-ray powder diffraction

The patterns show that the sample BRC2-M-dry is of a completely different type than all the others. The other five patterns show four weak signals which belong mainly to Goethite (FeOOH) and/or Ferrihyrite. The characteristic lines for Schwertmannite (JCPDF 47-1775) are indicated as green dashed lines with arrow in Figure 4. Except the line at a d-value of

0.157 nm, which is characteristic for most Fe (III) hydrolytic precipitates, no characteristic line for Schwertmannite can be recognized.

4.0 Conclusions:

The six selected samples for X-ray crystallography do not show hints on Schwertmannite (cf. Fig. 4). The considerations about the background of the phase diagram suggest that the use of this potential diagnostic approach to predict Schwertmannite formation is limited. From the comparison of predicted Schwertmannite solubilities on basis of two solubility products of this phase by Bigham et al. and Yu et al. (cf. Fig. 2) suggests, that these data are not significantly different if the uncertainty in chemical speciation is taken into account.

When calculating stability field diagrams as given in Fig. 1, the stability field of a solid phase is determined by the solubility products of all solid phases included in the diagram. Hence, the stability field given by Bigham et. al. in Fig. 1 is valid only for the mean value of the solubility product for Schwertmannite and the solubility products of the other phase's ferrihydrite, goethite and jarosite. The solubility products applied by Bigham et al. (Fig. 1) for these phases, however, are not the only values suggested in literature. Hence, using other values for these solubility products will result in different stability fields, and the formation of other iron minerals. In other words: the presence or absence of sulfate-bearing iron phases cannot be predicted on basis of the water analysis and some stability field diagram but must be investigated experimentally.

As often conclusions on mineral formation are made based on stability field diagram a potential concern raised with the sludge formation at South bay can be laid to rest. The accumulating iron-hydroxide sludges from the underground discharge at the mine site and in the Mud lake outflow area are unlikely to be a source of concern with respect to generating low pH. The sludges can therefore be considered stable and do not contribute to any further acidification of either Boomerang or Armanda Lake.

However it is recommended, that the tailings pore water chemistry is evaluated in detail, to define the potential for acidification, due to dissolution of secondary minerals. This work is in progress.

5.0 References:

1. Bigham J.M:, Schwertmann U., Traina S.J., Winland R.L., Wolf M. (1996) Geochimica Cosmochimica Acta 60: 2111- 2121

2. Yu J.-Y., Heo B., Chol I.-K., Cho J.-P., Chang H.-W. (1999) Geochimica Cosmochimica Acta 63: 3407 - 3416

3. Ödegaard-Jensen A., Ekberg C., Meinrath G. (2004) Talanta, in press
4. http://jess.murdoch.edu.au